JOURNAL OF GEOPHYSICAL RESEARCH, VOL. 111, A09101, doi:10.1029/2006JA011752, 2006

Hybrid simulations of parallel and oblique electromagnetic alpha/proton instabilities in the solar wind

Q. M. Lu,[1] L. D. Xia,[1] and S. Wang[1]

Received 29 March 2006; revised 31 May 2006; accepted 9 June 2006; published 6 September 2006.

[1] The linear Vlasov theory has shown that the relative flow between alpha particles and protons in the fast solar wind can excite both magnetosonic and oblique Alfven modes and the velocity threshold of the Alfven instability is lower than that of the magnetosonic instability. In this paper, hybrid simulations are performed to investigate the nonlinear evolution of parallel and oblique electromagnetic alpha/proton instabilities in the fast solar wind. The parallel proton plasma beta, defined as $b_{\|p} = 8pn_pk_BT_{\|p}/B_0^2$, is set equal to 0.15, and the initial average value of the alpha/proton relative flow speed is chosen as $1.76v_A$ (v_A is the local Alfven speed). The influences of the temperature anisotropy of alpha particles ($T_{\perp a}/T_{\|a}$) and temperature anisotropy of protons ($T_{\perp p}/T_{\|p}$) on the alpha/proton instabilities are also considered. The decrease of the temperature anisotropy of alpha particles ($T_{\perp a}/T_{\|a}$) can significantly enhance the amplitude of both the magnetosonic and oblique Alfven modes and decelerate alpha particles more efficiently, while the temperature anisotropy of protons ($T_{\perp p}/T_{\|p}$) tends to reduce the amplitudes of these two modes. Moreover, in the two-dimensional hybrid simulations the magnetosonic waves are first excited. Then the oblique Alfven waves are also excited and dominate the wave spectrum at the late stage of time evolution. The implications of our simulation results on observations in the fast solar wind are also discussed.

Citation: Lu, Q. M., L. D. Xia, and S. Wang (2006), Hybrid simulations of parallel and oblique electromagnetic alpha/proton instabilities in the solar wind, *J. Geophys. Res.*, *111*, A09101, doi:10.1029/2006JA011752.

1. Introduction

[2] In situ measurements have shown that there exist a variety of ion beams in the fast solar wind: a relative drift between two proton components (the core and beam protons), and a relative flow between minor ions such as alpha particles and the core protons [*Feldman et al.*, 1973a, 1973b, 1993, 1996; *Bame et al.*, 1975; *Marsch et al.*, 1982a, 1982b; *Marsch and Livi*, 1987; *Neugebauer et al.*, 1994, 1996; *Goldstein et al.*, 2000]. In general, the average relative velocity between the core and beam protons is parallel to the background magnetic field $\mathbf{B_0}$ with the drift velocity satisfying $1 \leq v_{pp}/v_A \leq 2$, where v_A is the local Alfven speed [*Goldstein et al.*, 2000; *Tu et al.*, 2004]. Among the minor ions in the fast solar wind, alpha particles are the most common species with an average abundance around 5% and flow faster than the core protons with an average relative drift velocity around the local Alfven speed [*Marsch et al.*, 1982a, 1982b; *Neugebauer et al.*, 1994, 1996].

[3] Electromagnetic instabilities excited by the proton beam have been extensively investigated with the linear Vlasov theory and hybrid simulations, and two distinct types of wave modes are found to be unstable for typical conditions of the fast solar wind [*Montgomery et al.*, 1975, 1976; *Marsch and Livi*, 1987; *Gary et al.*, 1985, 1986; *Leubner and Vinas*, 1986; *Gary*, 1991; *Winske and Omidi*, 1992; *Daughton and Gary*, 1998; *Daughton et al.*, 1999]. Besides the magnetosonic mode, several oblique Alfven modes can also be excited. The magnetosonic mode with maximum growth rate in the direction of the background magnetic field is more likely to grow at $b_{\|p} \geq 1$, and large-amplitude left-hand polarized waves in the solar wind are found to have important effects on the evolution of the magnetosonic waves [*Gomberoff*, 2003; *Araneda and Gomberoff*, 2004; *Kaghashvili et al.*, 2004]. The oblique Alfven modes tend to be excited at $b_{\|p} \ll 1$. However, due to the small concentrations of alpha particles and other minor ions in the solar wind, their contribution to electromagnetic waves is often ignored. Recently, the contribution of alpha particles to electromagnetic instabilities has been paid attentions [*Gary et al.*, 2000a, 2000b; *Li and Habbal*, 2000; *Gomberoff*, 2006], which is considered as one of mechanisms to decelerate alpha particles in the fast solar wind. Similar to proton/proton instabilities discussed above, both the magnetosonic and oblique Alfven modes can be excited by the alpha/proton instabilities. Using a cold plasma theory, *Gomberoff et al.* [1996] studied the velocity threshold of the magnetosonic mode excited by the alpha/proton instabilities. With the linear Vlasov theory, *Li and Habbal* [2000] showed that this threshold can be significantly reduced and the growth of the magnetosonic

[1]Chinese Academy of Sciences Key Laboratory of Basic Plasma Physics, School of Earth and Space Sciences, University of Science and Technology of China, Hefei, China.

0148-0227/06/2006JA011752$09.00

mode can be greatly enhanced when the temperature anisotropy of alpha particles ($T_{\perp a}/T_{\|a}$, where the subscripts $\perp$ and $\|$ denote the directions perpendicular and parallel to the background magnetic field, respectively) is less than 1. The nonlinear left-hand polarization waves are also found to have effects on the magnetosonic waves [*Gomberoff*, 2006]. With the linear Vlasov theory and two-dimensional hybrid simulations *Gary et al.* [2000a, 2000b] studied the electromagnetic alpha/proton instabilities in the fast solar wind, and found that both magnetosonic and oblique Alfven modes with properties similar to those of proton/proton instabilities are excited. The magnetosonic waves are dominated for large plasma beta, $b_{\|p}$ while the oblique Alfven waves operate when $b_{\|p} \ll 1$.

[4] In addition to ion beams, there also exist other nonthermal features in the fast solar wind. In general, the core protons tend to have a higher perpendicular temperature than parallel temperature, while alpha particles on average have a smaller perpendicular temperature than parallel temperature. The anisotropies of the core protons and alpha particles can be explained by scattering of ion cyclotron waves, which has been investigated by many authors [e.g., *Isenberg*, 1984; *Li and Habbal*, 1999; *Tu and Marsch*, 2001, 2002; *Hollweg and Isenberg*, 2002; *Ofman et al.*, 2002; *Lu and Wang*, 2005b]. In this paper, one-dimensional (1-D) and two-dimensional (2-D) hybrid simulations are carried out to study the nonlinear evolution of the parallel and oblique alpha/proton instabilities in the fast solar wind, in particular, the influences of the temperatures anisotropies of both protons and alpha particles.

[5] The paper is organized as follows: In section 2, we describe 1-D and 2-D hybrid simulation model. The simulation results are presented in section 3. The discussion and conclusions are given in section 4.

2. Simulation Model

[6] In hybrid simulations the ions are treated kinetically while the electrons are considered as a massless fluid [*Winske*, 1985]. The particles are advanced according to the well-known Boris algorithm while the electromagnetic fields are calculated with an implicit algorithm [*Lu and Wang*, 2005a]. The plasma is presumed to be collisionless, homogeneous, and magnetized, consisting of two ion components (protons and alpha particles) and the electron component. Their number densities are n_p, n_a and n_e, respectively. Initially, both protons and alpha particles are assumed to have a same thermal velocity in the direction parallel to the ambient magnetic field and to satisfy bi-Maxwellian velocity distribution with a drift speed (v_{0ap}) parallel to the background magnetic field.

[7] Periodic boundary conditions for the particles and fields are used in the simulations. Units of space and time are c/w_{pp} (where c/w_{pp} is the proton inertial length, c and w_{pp} are the light speed and proton plasma frequency, respectively) and W_p^{-1} (where $W_p = eB_0/m_p$ is the proton gyro frequency). We choose $n_a/n_e = 0.05$, and $b_{\|p} = 0.15$ if not stated explicitly. The initial drift speed between protons and alpha particles v_{0ap} is set as $1.76v_A$, which is parallel to the background magnetic field. The simulations are performed in the center-of-mass frame, where charge neutrality ($S_j e_j n_j = 0$) and the zero current condition ($S_j e_j n_j v_{0j} = 0$) are imposed at $t = 0$. The 1-D hybrid simulations are performed in the x direction. The background magnetic field is assumed to be $\mathbf{B}_0 = B_{x0}\hat{\mathbf{x}} + B_{y0}\hat{\mathbf{y}}$, and the angle between the x direction and background magnetic field is q = arctan B_{y0}/B_{x0}. The number of grid cells is $n_x = 256$, and the grid size is $\Delta x = 0.5\ c/w_{pp}$ with 300 particles per cell for each ion component. The time step is taken to be $W_p t = 0.04$. For 2-D hybrid simulations, the background magnetic field is along the x direction. The number of grid cells is $n_x \times n_y = 256 \times 128$, and the grid size is $\Delta x = 0.5\ c/w_{pp}$ and $\Delta y = 1.0\ c/w_{pp}$, with 36 particles per cell for each ion component. The time step is $W_p t = 0.04$, which is the same as in the 1-D hybrid simulations.

3. Simulation Results

[8] The linear Vlasov theory has predicted that only magnetosonic mode can be excited by parallel alpha/proton instabilities, while both magnetosonic and Alfven modes can be excited by oblique alpha/proton instabilities [*Gary et al.*, 2000a]. In this paper with 1-D and 2-D hybrid simulations we investigate the nonlinear evolution of the parallel and oblique alpha/proton instabilities, and the effects of the proton plasma beta, the temperature anisotropies of protons and alpha particles are also considered. Three sets of parameters are used: (1) $T_{\perp a}/T_{\|a} = 1.0$, $T_{\perp p}/T_{\|p} = 1.0$, (2) $T_{\perp a}/T_{\|a} = 0.6$, $T_{\perp p}/T_{\|p} = 1.0$, and (3) $T_{\perp a}/T_{\|a} = 1.0$, $T_{\perp p}/T_{\|p} = 2.0$. In the following, we first describe the parallel and oblique alpha/proton instabilities with 1-D hybrid simulations, and then we show the results of 2-D hybrid simulations.

3.1. Parallel Alpha/Proton Instabilities With θ = 0

[9] The linear Vlasov theory shows that magnetosonic waves are unstable in the parallel alpha/proton instabilities. The growth rate of the waves decreases with the increase of the temperature anisotropy of protons [*Gary et al.*, 2000b; *Araneda et al.*, 2002], while it is enhanced significantly with the decrease of the temperature anisotropy of alpha particles [*Li and Habbal*, 2000; *Gary et al.*, 2000b]. Figure 1 shows the time evolution of the amplitude of the fluctuating magnetic field (Figure 1a), the relative drift velocity between protons and alpha particles (Figure 1b), the temperature anisotropy of alpha particles ($T_{\perp a}/T_{\|a}$) (Figure 1c), and the temperature anisotropy of protons ($T_{\perp p}/T_{\|p}$) (Figure 1d) for case A, $T_{\perp a}/T_{\|a} = 1.0$, $T_{\perp p}/T_{\|p} = 1.0$; case B, $T_{\perp a}/T_{\|a} = 0.6$, $T_{\perp p}/T_{\|p} = 1.0$; and case C, $T_{\perp a}/T_{\|a} = 1.0$, $T_{\perp p}/T_{\|p} = 2.0$. Consistent with the results of the linear theory, from Figure 1, one finds that the inverse temperature anisotropy of alpha particles can significantly enhance the amplitude of the fluctuating magnetic field, while the temperature anisotropy of protons reduces the amplitude of the magnetosonic waves. In case A, the magnetosonic waves begin to grow at about $W_p t = 50$, and at about $W_p t = 100$ they reach their maximum amplitude of about $dB^2/B_0^2 = 0.006$. A quasi-equilibrium stage is attained at about $W_p t = 250$ with the amplitude of about $dB^2/B_0^2 = 0.0006$. In case B, the maximum amplitude of the magnetosonic waves and the amplitude at the quasi-equilibrium stages are about $dB^2/B_0^2 = 0.014$ and 0.0018, respectively. In case C, the maximum amplitude of the magnetosonic waves and the amplitude at the

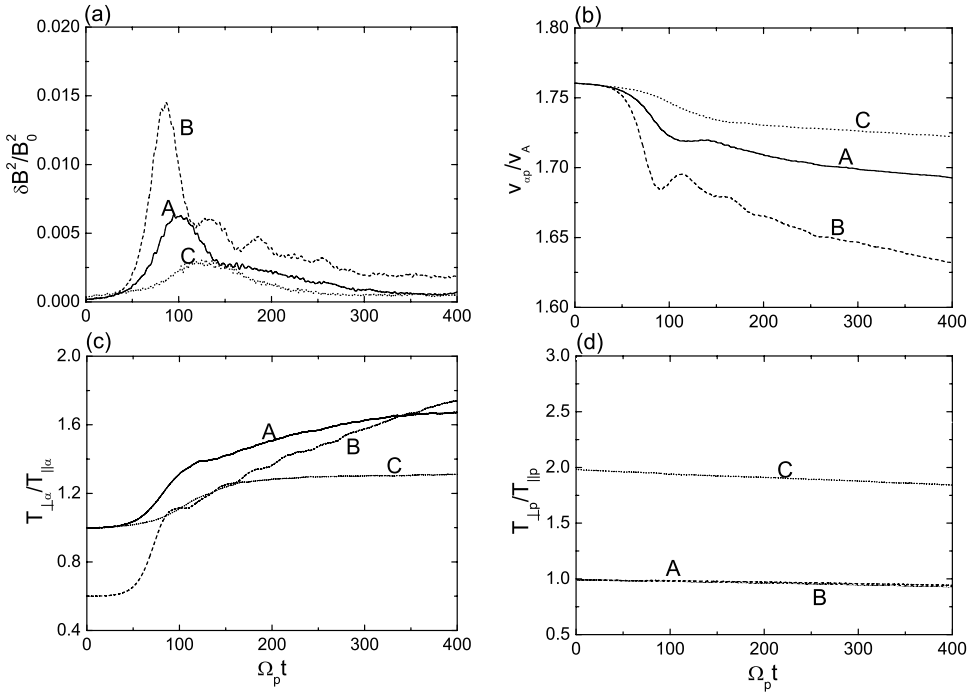

Figure 1. Time evolution of (a) the amplitude of the fluctuating magnetic field (dB^2/B_0^2), (b) the relative velocity between protons and alpha particles (v_{ap}/v_A), (c) the temperature anisotropy of alpha particles ($T_{\perp a}/T_{\|a}$), and (d) the temperature anisotropy of protons ($T_{\perp p}/T_{\|p}$). The results are obtained from 1-D hybrid simulations of the parallel alpha/proton instabilities. The solid, dashed, and dotted lines represent case A, $T_{\perp a}/T_{\|a} = 1.0$, $T_{\perp p}/T_{\|p} = 1.0$; case B, $T_{\perp a}/T_{\|a} = 0.6$, $T_{\perp p}/T_{\|p} = 1.0$; and case C, $T_{\perp a}/T_{\|a} = 1.0$, $T_{\perp p}/T_{\|p} = 2.0$, respectively.

quasi-equilibrium stages are $dB^2/B_0^2 = 0.0025$ and 0.0004, respectively. Correspondingly, with the excitation of the magnetosonic waves, the relative velocity between protons and alpha particles decreases, while the temperature anisotropy of alpha particles increases. At the quasi-equilibrium stage, the relative velocities for cases A, B, and C are about $1.69v_A$, $1.63v_A$, and $1.72v_A$, respectively, while the temperature anisotropies of alpha particles are about 1.67, 1.74, and 1.3, respectively. The magnetosonic waves have no effect on the proton temperature anisotropy because they cannot

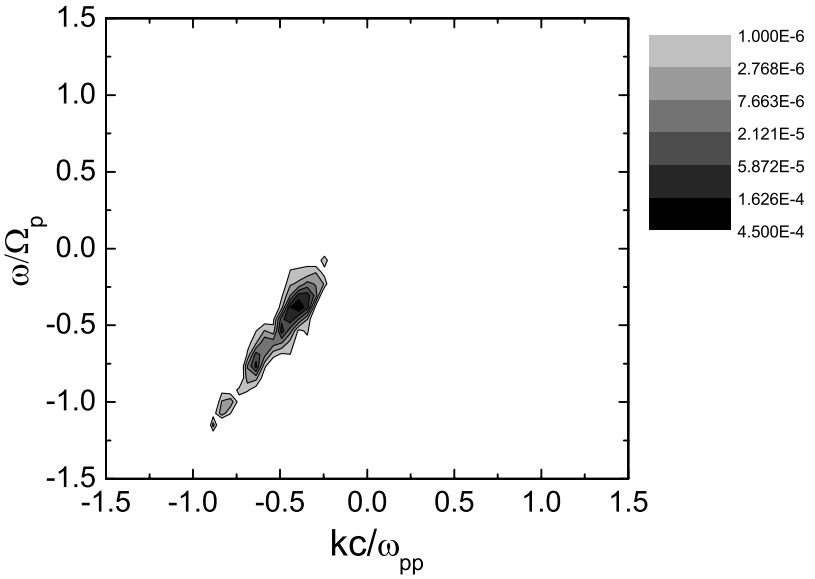

Figure 2. Characteristics of $w-k$ diagram obtained by FFT transforming B_y from $W_pt = 48.0$ to $W_pt = 129.92$ for case B. The results are obtained from 1-D hybrid simulations of the parallel alpha/proton instabilities. Note that the magnetosonic waves propagating to $+x$ and $-x$ direction reside in the first and second quadrants, respectively, while the Alfven waves propagating to $+x$ and $-x$ direction reside in the third and fourth quadrants, respectively.

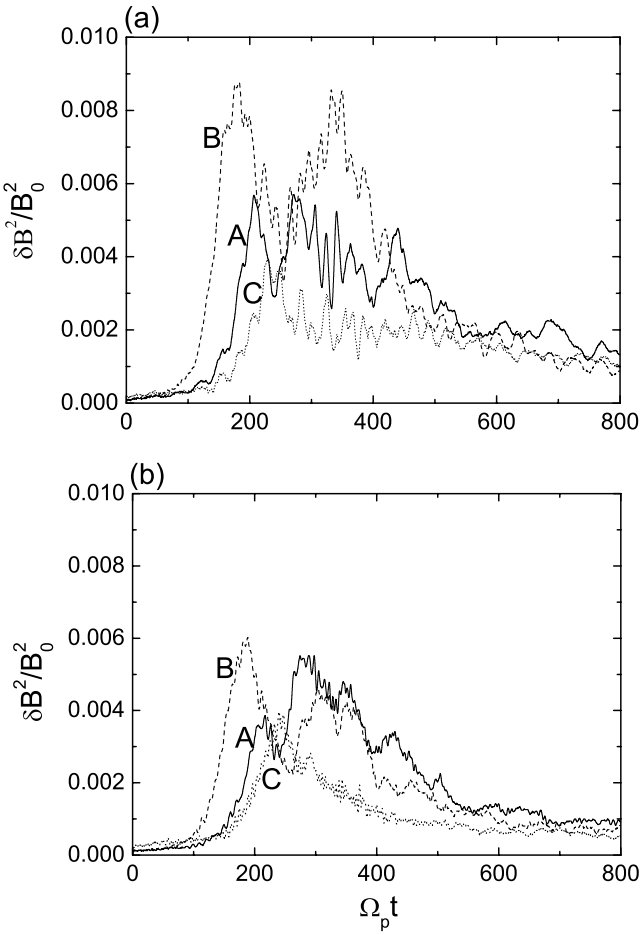

Figure 3. Time evolution of the amplitude of (a) the magnetosonic waves and (b) the Alfven waves. The results are obtained from 1-D hybrid simulations of the oblique alpha/parallel instabilities. The solid, dashed and dotted lines represent case A, $T_{\perp a}/T_{\|a} = 1.0$, $T_{\perp p}/T_{\|p} = 1.0$; case B, $T_{\perp a}/T_{\|a} = 0.6$, $T_{\perp p}/T_{\|p} = 1.0$; and case C, $T_{\perp a}/T_{\|a} = 1.0$, $T_{\perp p}/T_{\|p} = 2.0$, respectively.

resonantly interact with protons. If we further increase the proton temperature anisotropy, the ion cyclotron waves will also be excited, which can heat alpha particles. Such phenomena have already been studied by many authors [e.g., *Araneda et al.*, 2002; *Gary et al.*, 2003; *Lu and Wang*, 2005a, 2006; *Lu et al.*, 2006], which are beyond the scope of this paper. Figure 2 describes the characteristics of $w-k$ diagram obtained by fast Fourier transforming (FFT) B_y from $W_p t = 48.0$ to $W_p t = 129.92$ for case B. It is found that only the magnetosonic waves which propagate to the $+x$ direction are excited, and the frequency ranges from $0.2W_p$ to $0.7W_p$.

3.2. Oblique Alpha/Proton Instabilities With θ = 30

[10] The oblique alpha/proton instabilities are unstable to both the magnetosonic and Alfven waves. With the methods developed by *Terasawa et al.* [1986], we can separate the wave fluctuations into positive and negative helical parts. For positive helicity, forward propagating waves will be right-hand polarized (magnetosonic waves), whereas waves propagating backward will be left-hand polarized (Alfven waves). Similarly, forward propagating waves with negative helicity will be left-hand polarized (Alfven waves), whereas the backward propagating ones will be right-hand polarized (magnetosonic waves). In our simulations, both the positive

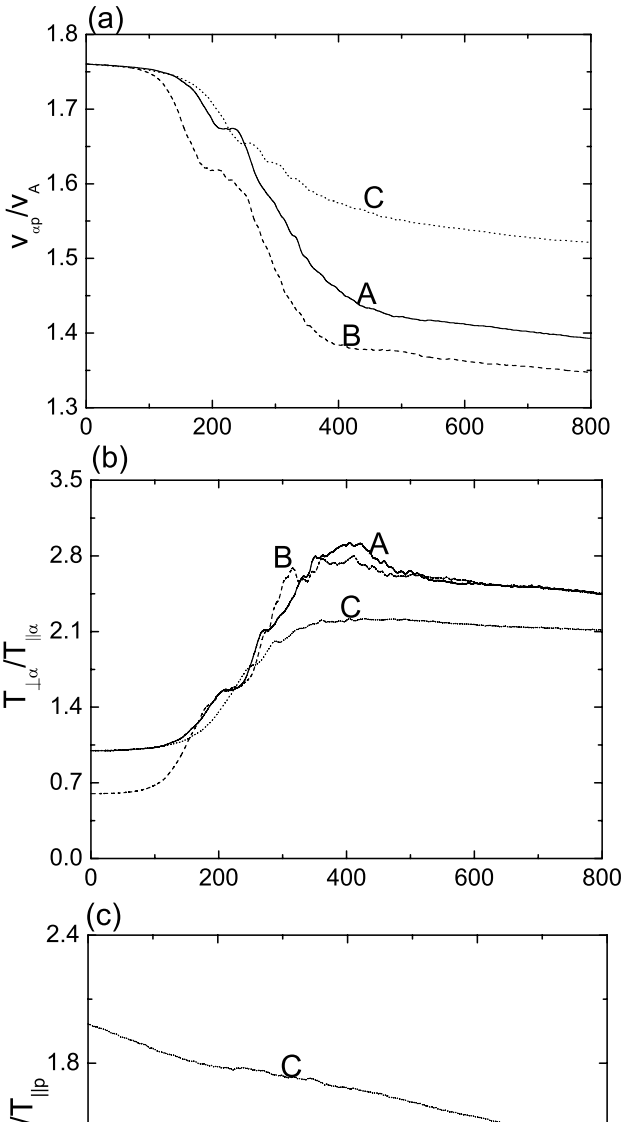

Figure 4. Time evolution of (a) the relative velocity between protons and alpha particles (v_{ap}/v_A), (b) the temperature anisotropy of alpha particles ($T_{\perp a}/T_{\|a}$), and (c) the temperature anisotropy of protons ($T_{\perp p}/T_{\|p}$). The results are obtained from 1-D hybrid simulations of the oblique alpha/proton instabilities. The solid, dashed and dotted lines represent case A, $T_{\perp a}/T_{\|a} = 1.0$, $T_{\perp p}/T_{\|p} = 1.0$; case B, $T_{\perp a}/T_{\|a} = 0.6$, $T_{\perp p}/T_{\|p} = 1.0$; and case C, $T_{\perp a}/T_{\|a} = 1.0$, $T_{\perp p}/T_{\|p} = 2.0$, respectively.

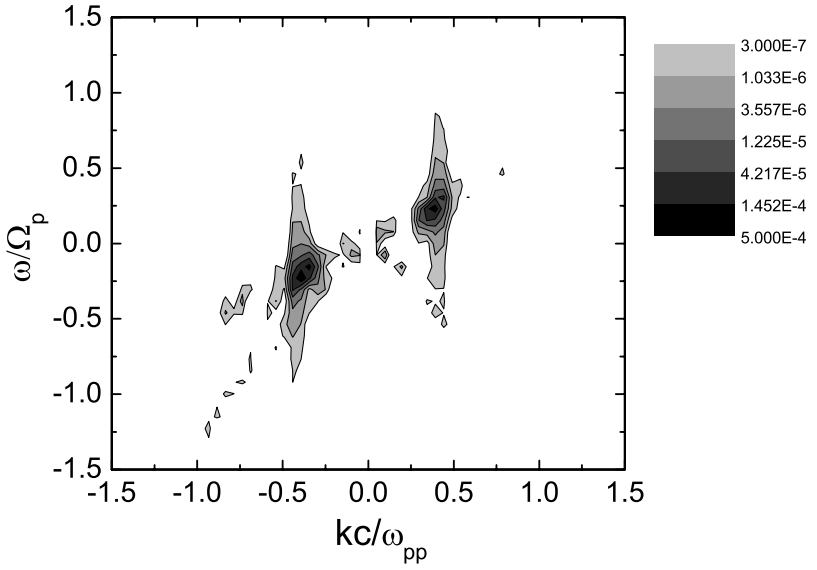

Figure 5. Characteristics of $w-k$ diagram obtained by FFT transforming B_y from $W_pt = 100.0$ to $W_pt = 181.92$ for case B. The results are obtained from 1-D hybrid simulations of the oblique alpha/proton instabilities. Note that the magnetosonic waves propagating to $+x$ and $-x$ direction reside in the first and second quadrants, respectively, while the Alfven waves propagating to $+x$ and $-x$ direction reside in the third and fourth quadrants, respectively.

and negative helical fluctuations propagate forward, which correspond to magnetosonic waves and Alfven waves, respectively. Figure 3 describes the time evolution of the amplitudes of the magnetosonic waves (Figure 3a) and the Alfven waves (Figure 3b) for case A, $T_{\perp a}/T_{\|a} = 1.0$, $T_{\perp p}/T_{\|p} = 1.0$; case B, $T_{\perp a}/T_{\|a} = 0.6$, $T_{\perp p}/T_{\|p} = 1.0$; and case C, $T_{\perp a}/T_{\|a} = 1.0$, $T_{\perp p}/T_{\|p} = 2.0$. With the linear Vlasov theory, *Daughton and Gary* [1998] found that in oblique proton/proton instabilities the Alfven waves are also unstable, and the temperature anisotropy of either protons or alpha particles reduces the growth rate. Similar to the oblique proton/proton instabilities, our results show that in the oblique alpha/proton instabilities the inverse temperature anisotropy of alpha particles can enhance the amplitude of both the magnetosonic waves and oblique Alfven waves. The temperature anisotropy of protons tends to reduce the amplitude of the magnetosonic and Alfven waves. The maximum amplitudes which the magnetosonic waves can attain for cases A, B, and C are $dB^2/B_0^2 = 0.006$, 0.009, and 0.004, and the corresponding amplitudes at the quasi-equilibrium stage are $dB^2/B_0^2 = 0.0012$, 0.0010, and 0.0010. The maximum amplitudes that the Alfven waves can attain for cases A, B, and C are $dB^2/B_0^2 = 0.006$, 0.006, 0.004, and the corresponding amplitudes at the quasi-equilibrium stage are $dB^2/B_0^2 = 0.0009$, 0.0008, 0.0006. Figure 4 shows the time evolution of the relative velocity between protons and alpha particles (v_{ap}) (Figure 4a), the temperature anisotropy of alpha particles ($T_{\perp a}/T_{\|a}$) (Figure 4b), and the temperature anisotropy of protons ($T_{\perp p}/T_{\|p}$) (Figure 4c) for cases A, B, and C, respectively. Their evolution is due to the combined effects of both the magnetosonic waves and Alfven waves. The deceleration of alpha particles can be thought to consist of two stages. For example in case A, first the relative velocity between protons and particles (v_{ap}) decreases from $1.76v_A$ to $1.67v_A$ due to scattering of the magnetosonic waves, and then it is decelerated from $1.67v_A$ to $1.39v_A$ due to scattering of the oblique Alfven waves. At the quasi-equilibrium stage, the relative velocities for cases A, B, and C are about $1.39v_A$, $1.35v_A$, and $1.52v_A$, respectively, which is much smaller than the corresponding values of the parallel alpha/proton instabilities. The reason is that the oblique Alfven waves have lower velocity threshold than that of the magnetosonic waves, which has been demonstrated by *Gary et al.* [2000a]. The oblique alpha/proton instabilities also have little effect on the proton temperature, but it can scatter alpha particles into much higher temperature anisotropy than the parallel alpha/proton instabilities can do.

[11] After separating the magnetic fluctuations into two parts corresponding to the magnetosonic waves and Alfven waves, the $w-k$ diagram can be obtained by FFT transforming the two parts. Figure 5 describes the characteristics of $w-k$ diagram obtained by FFT transforming B_y^+ and B_y^- (where B_y^+ and B_y^- are the magnetic fluctuations corresponding to the magnetosonic waves and Alfven waves) from $W_pt = 100.0$ to $W_pt = 181.92$ for case B. The waves reside in the first and third quadrants are the Alfven waves and magnetosonic waves, respectively. Both the magnetosonic waves and Alfven waves propagate to the $+x$ direction, and their dominant frequencies are concentrated near $0.2W_p$ and $0.25W_p$.

[12] We also consider the effects of the proton plasma beta ($b_{\|p}$) on the oblique alpha/proton instabilities. Figure 6a describes the time evolution of the amplitude of the oblique Alfven waves, and Figure 6b describes the relative velocity between alpha particles and protons (v_{ap}/v_A) for different proton plasma beta ($b_{\|p}$). From Figure 6, we are able to find that with the decrease of $b_{\|p}$, the amplitude of the oblique Alfven waves increases. For example, in case of $b_{\|p} = 0.15$ (line denoted by B) and $b_{\|p} = 0.05$ (line denoted by E),

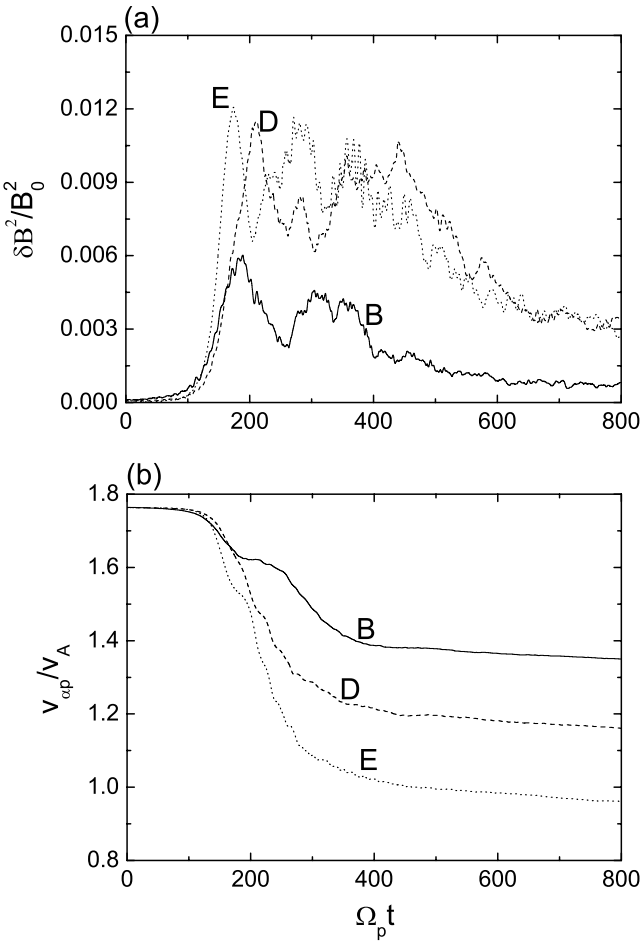

Figure 6. Time evolution of (a) the amplitude of the oblique Alfven waves and (b) the relative velocity between alpha particles and protons (v_{ap}/v_A) for (B) $b_{\|p}$ = 0.15, (D) $b_{\|p}$ = 0.10 and (E) $b_{\|p}$ = 0.05. $T_{\perp a}/T_{\|a}$ and $T_{\perp p}/T_{\|p}$ are set to 0.6 and 1.0, respectively. The solid, dashed and dotted lines represent different plasma beta: (B), $b_{\|p}$ = 0.15; (D), $b_{\|p}$ = 0.10; and (E), $b_{\|p}$ = 0.05, respectively. The results are obtained from 1-D hybrid simulations of the oblique Alfven alpha/proton instabilities.

the maximum amplitudes of the Alfven waves are about dB^2/B_0^2 = 0.006 and dB^2/B_0^2 = 0.012, respectively. Therefore alpha particles can be decelerated more efficiently when $b_{\|p}$ decreases. When $b_{\|p}$ = 0.05, at the quasi-equilibrium stage the relative velocity between alpha particles and protons can even be decelerated to near the local Alfven speed. At the quasi-equilibrium stage, the relative velocities for cases B, D, and E are about 1.35v_A, 1.16v_A, and 0.97v_A, respectively.

3.3. Two-Dimensional Hybrid Simulations of the Alpha/Proton Instabilities

[13] In this subsection, we describe the case B with 2-D hybrid simulations. The parameters are $T_{\perp a}/T_{\|a}$ = 0.6, $T_{\perp p}/T_{\|p}$ = 1.0, and $b_{\|p}$ = 0.15. Figure 7 shows the time evolution of the relative velocity between alpha particles and protons v_{ap}/v_A. Similar to the results of 1-D hybrid simulations, alpha particles are first decelerated by the magnetosonic waves, and then are further decelerated to about v_{ap} = 1.38v_A at the quasi-equilibrium stage by the oblique Alfven waves. Figure 8 describes the characteristics of $k_x - k_y$ diagram at different time $W_p t$ = 100 (Figure 8a), $W_p t$ = 150 (Figure 8b), $W_p t$ = 300 (Figure 8c), and $W_p t$ = 800 (Figure 8d). It shows that the parallel magnetosonic waves are first excited. At $W_p t$ = 100, the wave numbers concentrate near (k_x, k_y) = (0.56 w_{pp}/c, 0.0). At the same time, the average velocity of alpha particles is decelerated to about 1.65v_A by the magnetosonic waves. From about $W_p t$ = 150, besides the parallel magnetosonic waves, the oblique Alfven waves begin to be excited, and they further decelerate alpha particles. At about $W_p t$ = 300, the Alfven waves become more important than the magnetosonic waves. Furthermore, the magnetosonic waves almost disappear and only the Alfven waves remain at the quasi-equilibrium stage. We have also found $k_y/k_x \approx 0.6$ for the Alfven waves, i.e., the Alfven waves propagate obliquely with a propagation angle of about 31, which is consistent with our 1-D hybrid simulations of the oblique alpha/proton instabilities.

4. Discussion and Conclusions

[14] Observations in the fast solar wind showed that the relative flow speed between alpha particles and protons is fairly constant beyond 0.3 AU, while the local Alfven speed decreases from about 150 km/s at 0.3 AU to 30 $\sim$ 50 km/s at 1 AU. Therefore a significant fraction of the kinetic energy of alpha particles should be released when they flow from the solar corona into interplanetary space. Electromagnetic alpha/proton instabilities are suggested to be the most possible mechanism for this kind of energy release. The magnetosonic waves excited by the alpha/proton instabilities have been thoroughly investigated [*Li and Habbal*, 2000; *Gary et al.*, 2000b; *Gomberoff*, 2006] in order to account for the deceleration mechanism. *Gary et al.* [2000a] found that besides the magnetosonic waves the oblique Alfven waves with lower velocity threshold are also unstable when $b_{\|p} \ll 1$ in the solar wind. In this paper, we investigate the nonlinear evolution of the parallel and oblique alpha/proton instabilities using 1-D and 2-D hybrid

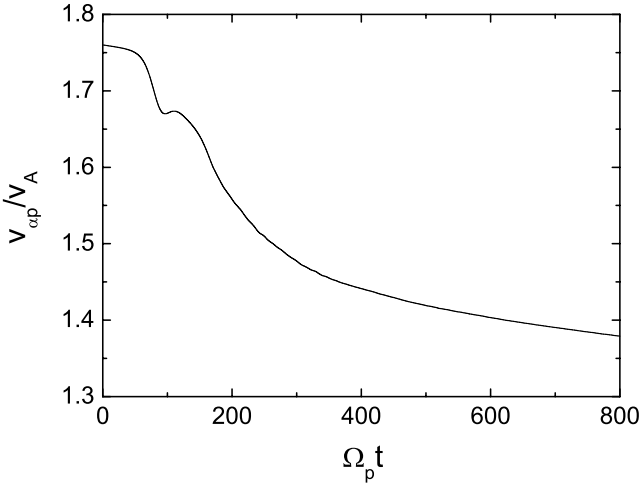

Figure 7. Time evolution of the relative velocity between alpha particles and protons v_{ap}/v_A for case B. The results are obtained from 2-D hybrid simulations.

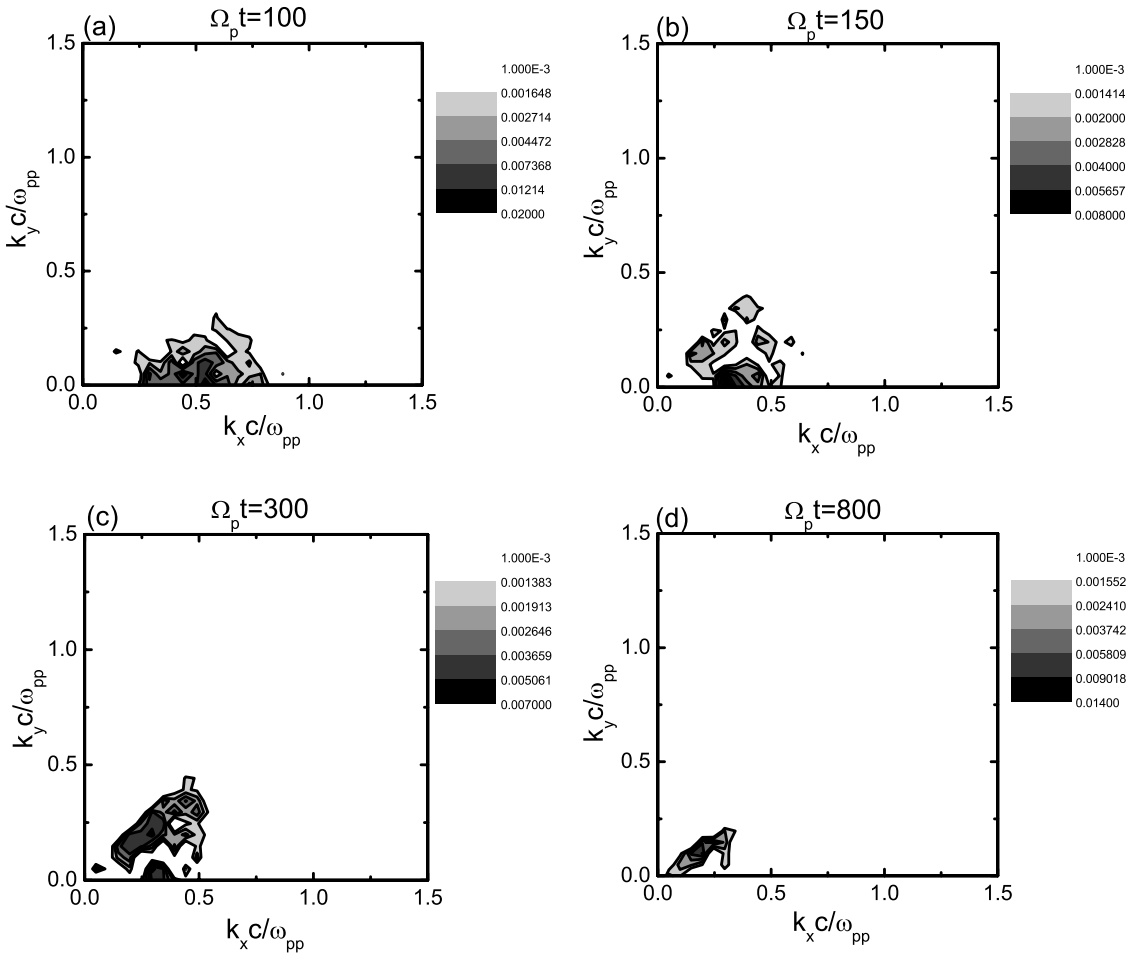

Figure 8. Characteristics of $k_x - k_y$ diagram obtained from the FFT transforming B_y at different time (a) W_pt = 100, (b) W_pt = 150, (c) W_pt = 300 and (d) W_pt = 800 for case B. The results are obtained from 2-D hybrid simulations.

simulations. Consistent with the linear Vlasov theory [*Gary et al.*, 2000a], our simulations confirm that both the magnetosonic and oblique Alfven can be excited, while the oblique Alfven waves can decelerate alpha particles into much smaller average velocity. We also take into account the effects of the temperature anisotropies of alpha and proton particles on the alpha/proton instabilities in 1-D hybrid simulations. When the temperature anisotropy of alpha particles ($T_{\perp a}/T_{\|a}$) is less than 1, the amplitudes of both the magnetosonic waves and oblique Alfven waves are enhanced, and thus decelerate alpha particles more efficiently. The temperature anisotropy of protons will reduce the amplitudes of both the magnetosonic waves and oblique Alfven waves, and thus decelerates alpha particles with less efficiency.

[15] In order to obtain substantial growth rates, we initialized our simulations with v_{0ap}/v_A = 1.76, which is larger than the typical value observed in the solar wind. Alpha particles are first decelerated by the magnetosonic waves, and then are further decelerated by the oblique Alfven waves. The velocity threshold of the oblique Alfven instability is much lower than that of the magnetosonic instability. In the real situation of the fast solar wind, the relative drift between protons and alpha particles is always near the threshold for electromagnetic instabilities. Therefore the most possible waves excited by alpha/proton instabilities in the fast solar wind when $b_{\|p} \ll 1$, which is also the most possible mechanism to release the kinetic energy of alpha particles, should be the oblique Alfven waves due to their lower velocity threshold. Indeed, in our 1-D hybrid simulation, alpha particles can be decelerated to near the Alfven speed when $b_{\|p}$ = 0.05. Meanwhile, 2-D hybrid simulations show that the magnetosonic waves are first excited in the alpha/proton instabilities, and then the oblique Alfven waves. At the late stage of time evolution the Alfven waves dominate the wave spectrum and further decelerate alpha particles to much low velocity.

[16] **Acknowledgments.** This research was supported by Program for New Century Excellent Talents in University (NCET) and the National Science Foundation of China (NSFC) under grants 40304012 and 40336052.

[17] Zuyin Pu wishes to thank S. Peter Gary and Luis Gomberoff for their assistance in evaluating this paper.

References

Araneda, J. A., and L. Gomberoff (2004), Stabilization of right-hand polarized beam plasma instabilities due to a large-amplitude left-hand polarized wave: A simulation study, *J. Geophys. Res.*, *109*, A01106, doi:10.1029/2003JA010189.

Araneda, J. A., A. F. Vinas, and H. F. Astudillo (2002), Proton core tem-

perature effects on the relative drift and anisotropy evolution of the ion beam instability in the fast solar wind, *J. Geophys. Res.*, *107*(A12), 1453, doi:10.1029/2002JA009337.

Bame, S. J., J. R. Asbridge, W. C. Feldman, S. P. Gary, and M. D. Montgomery (1975), Evidence for local ion heating in solar wind high speed streams, *Geophys. Res. Lett.*, *9*, 373–375.

Daughton, W., and S. P. Gary (1998), Electromagnetic proton/proton instabilities in the solar wind, *J. Geophys. Res.*, *103*, 20,613–20,620.

Daughton, W., S. P. Gary, and D. Winske (1999), Electromagnetic proton/proton instabilities in the solar wind: Simulations, *J. Geophys. Res.*, *104*, 4657–4668.

Feldman, W. C., J. R. Asbridge, S. J. Bame, and M. D. Montgomery (1973a), Double ion streams in the solar wind, *J. Geophys. Res.*, *78*, 2017–2027.

Feldman, W. C., J. R. Asbridge, S. J. Bame, and M. D. Montgomery (1973b), On the origin of solar wind proton thermal anisotropy, *J. Geophys. Res.*, *78*, 6451–6468.

Feldman, W. C., J. T. Gosling, D. J. McComas, and J. L. Phillips (1993), Evidence for ion jets in the high-speed solar wind, *J. Geophys. Res.*, *98*, 5593–5606.

Feldman, W. C., B. L. Barraclough, J. L. Philips, and Y. M. Wang (1996), Constraint on high-speed solar wind structure near its coronal base: A Ulysses perspective, *Astron. Astrophys.*, *316*, 355–367.

Gary, S. P. (1991), Electromagnetic ion/ion instabilities and their consequences in space plasmas: A review, *Space Sci. Rev.*, *56*, 373–415.

Gary, S. P., C. D. Madland, and B. T. Tsurutani (1985), Electromagnetic ion beam instabilities, *Phys. Fluids*, *28*, 3691–3695.

Gary, S. P., C. D. Madland, D. Schriver, and D. Winske (1986), Computer simulations of electromagnetic cool ion beam instabilities, *J. Geophys. Res.*, *91*, 4188–4196.

Gary, S. P., L. Yin, D. Winske, and D. B. Reisenfeld (2000a), Electromagnetic alpha/proton instabilities in the solar wind, *Geophys. Res., Lett.*, *27*, 1355–1358.

Gary, S. P., L. Yin, D. Winske, and D. B. Reisenfeld (2000b), Alpha/proton magnetosonic instability in the solar wind, *J. Geophys. Res.*, *105*, 20,989–20,996.

Gary, S. P., L. Yin, D. Winske, L. Ofman, B. E. Goldstein, and M. Neugebauer (2003), Consequences of proton and alpha anisotropies in the solar wind: Hybird simulations, *J. Geophys. Res.*, *108*(A2), 1068, doi:10.1029/2002JA009654.

Goldstein, B., M. Neugebauer, L. D. Zhang, and S. P. Gary (2000), Observed constrains on proton-proton relative velocity in the solar wind, *Geophys. Res., Lett.*, *27*, 53–56.

Gomberoff, L. (2003), Stabilization of linear ion beam right-hand polarization instabilities by nonlinear Alfven/ion-cyclotron waves, *J. Geophys. Res.*, *108*(A6), 1261, doi:10.1029/2003JA009837.

Gomberoff, L. (2006), Effect of nonlinear circularly polarized waves on linear instabilities triggered by an alpha particle beam, *J. Geophys. Res.*, *111*, A02101, doi:10.1029/2005JA011407.

Gomberoff, L., G. Gnavi, and F. T. Gratton (1996), Minor heavy ion electromagnetic beam-plasma interactions in the solar wind, *J. Geophys. Res.*, *101*, 13,517–13,522.

Hollweg, J. V., and P. A. Isenberg (2002), Generation of the fast solar wind: A review with emphasis on the resonant cyclotron interaction, *J. Geophys. Res.*, *107*(A7), 1147, doi:10.1029/2001JA000270.

Isenberg, P. A. (1984), Resonant acceleration and heating of solar wind ions: Anisotropy and dispersion, *J. Geophys. Res.*, *89*, 6613–6622.

Kaghashvili, E. K., B. J. Vasquez, G. P. Zank, and J. V. Hollweg (2004), Deceleration of relative streaming between proton components among nonlinear low-frequency Alfven waves, *J. Geophys. Res.*, *109*, A12101, doi:10.1029/2004JA010382.

Leubner, M. P., and A. F. Vinas (1986), Stability analysis of double-peaked proton distribution functions in the solar wind, *J. Geophys., Res.*, *91*, 13,366–13,372.

Li, X., and S. R. Habbal (1999), Ion cyclotron waves, instabilities and solar wind heating, *Sol. Phys.*, *190*, 485–497.

Li, X., and S. R. Habbal (2000), Proton/alpha magnetosonic instability in the fast solar wind, *J. Geophys. Res.*, *105*, 7483–7489.

Lu, Q. M., and S. Wang (2005a), Formation of He^{2+} shell-like distributions downstream of the earth's bow shock, *Geophys. Res. Lett.*, *32*, L03111, doi:10.1029/2004GL021508.

Lu, Q. M., and S. Wang (2005b), Proton and He^{2+} temperature anisotropies in the solar wind driven by ion cyclotron waves, *Chin. J. Astron. Astrophys.*, *5*, 184–192.

Lu, Q. M., and S. Wang (2006), Electromagnetic waves downstream of quasi-perpendicular shocks, *J. Geophys. Res.*, *111*, A05204, doi:10.1029/2005JA011319.

Lu, Q. M., F. Guo, and S. Wang (2006), Magnetic spectral signatures in the terrestrial plasma depletion layer: Hybrid simulations, *J. Geophys. Res.*, *111*, A04207, doi:10.1029/2005JA011405.

Marsch, E., and S. Livi (1987), Observational evidence for marginal stability of solar wind, *J. Geophys. Res.*, *92*, 7263–7268.

Marsch, E., K. H. Muhlhauser, H. Rosenbauer, R. Schwenn, and F. M. Neubauser (1982a), Solar wind helium ions: Observations of the Helios solar probes between 0.3 and 1 AU, *J. Geophys. Res.*, *87*, 35–51.

Marsch, E., K. H. Muhlhauser, R. Schwenn, H. Rosenbauer, W. Pilipp, and F. M. Neubauer (1982b), Solar wind protons: Three-dimensional velocity distributions and derived plasma parameters measured between 0.3 and 1 AU, *J. Geophys. Res.*, *87*, 52–72.

Montgomery, M. D., S. P. Gary, D. W. Dorslund, and W. C. Feldman (1975), Electromagnetic ion-beam instabilities in the solar wind, *Phys. Rev. Lett.*, *35*, 667–670.

Montgomery, M. D., S. P. Gary, W. C. Feldman, and D. W. Forslund (1976), Electromagnetic instabilities driven by unequal proton beams in the solar wind, *J. Geophys. Res.*, *81*, 2743–2749.

Neugebauer, M., B. E. Goldstein, S. J. Bame, and W. C. Feldman (1994), Ulysses near-ecliptic observations of differential flow between protons and alphas in the solar wind, *J. Geophys. Res.*, *99*, 2505–2511.

Neugebauer, M., B. E. Goldstein, E. J. Smith, and W. C. Feldman (1996), Ulysses observations of differential alpha-proton streaming in the solar wind, *J. Geophys. Res.*, *101*, 17,047–17,055.

Ofman, L., S. P. Gary, and A. Vinas (2002), Resonant heating and acceleration of ions in coronal holes driven by cyclotron resonant spectra, *J. Geophys. Res.*, *107*(A12), 1461, doi:10.1029/2002JA009432.

Terasawa, T., M. Hoshino, J. Sakai, and T. Hada (1986), Decay instability of finite-amplitude circularly polarized Alfven waves: A numerical simulation of stimulated Brillouin scattering, *J. Geophys. Res.*, *91*, 4171–4181.

Tu, C. Y., and E. Marsch (2001), On cyclotron wave heating and acceleration of solar wind ions in the outer corona, *J. Geophys. Res.*, *106*, 8233–8252.

Tu, C. Y., and E. Marsch (2002), Anisotropy regulation and plateau formation through pitch angle diffusion of solar wind protons in resonance with cyclotron waves, *J. Geophys. Res.*, *107*(A9), 1249, doi:10.1029/2001JA000150.

Tu, C. Y., E. Marsch, and Z. R. Qin (2004), Dependence of the proton beam drift velocity on the proton core plasma beta in the solar wind, *J. Geophys. Res.*, *109*, A05101, doi:10.1029/2004JA010391.

Winske, D. (1985), Hybird simulation codes with applications to shocks and upstream waves, *Space Sci. Rev.*, *42*, 53–66.

Winske, D., and N. Omidi (1992), Electromagnetic ion/ion cyclotron instability: Theory and simulations, *J. Geophys. Res.*, *97*, 14,779–14,799.

Q. M. Lu, S. Wang, and L. D. Xia, CAS Key Laboratory of Basic Plasma Physics, School of Earth and Space Sciences, University of Science and Technology of China, Hefei, Anhui 230026, China. (qmlu@ustc.edu.cn)